A Model of Heave Dynamics for Bagged Air Cushioned Vehicles

Jared Miller[1], Bahram Shafai[1]

Abstract— **This paper presents a simple model of the heave dynamics of an air cushioned vehicle. A set of nonlinear differential equations are extended to the case of a bagged vehicle, which show the Forchheimer porosity approximation matching physically observed results. The model exhibits stability under atmospheric pressure, and a tendency towards instability in near-vacuum conditions. Inner estimates of regions of attractions are found to verify stability in atmosphere, and track simulation shows system disturbance rejection under a drifting road height and gaps.**

I. INTRODUCTION

Air Cushioned Vehicles (ACV) are crafts that are supported underneath by a 'cushion' of pressurized air [1]. This cushion helps insulate the vehicle against wave breaks and ground disturbances, and generally leads to a smooth and more reliable ride. The two main mechanisms of creating an air cushion are through plenum chambers and peripheral jets [2]. Plenum chambers are cavities of pressurized air directly underneath the vehicle, in which the bottom may be closed off by a bag or left open with a skirt. Variations of this concept exist including the bag-and-fingers approach, where the bag is split into a series of triangular segments from a common chamber. The peripheral jet sends an angled stream of air from the top of the skirt, and the resulting curtain will form a cushion underneath the vehicle. Air Cushioned Vehicles are robust craft that can be used for diverse applications such as landing on rough terrain, tendering, transport of heavy payload and passengers, and racing. Steering is performed by applying external forces with methods such as fans, impellers, and jet engines. Their operating principles were first formulated and optimized by Sir Christopher Cockerell in 1955, and further research of hovercraft physics continued from the 1960-80s [3].

Some objectives behind ACV optimization include reducing oscillations to smooth out a ride (heave instabilities), robustifying the system against external disturbances (such as waves), increasing maneuverability, and reducing the airflow/power needed to maintain the cushion. These optimization objectives first require a model of ACV motion. Hinchey identified several nonlinearities in air-cushioned dynamics in 1981, which include the fan's pressure-volume relationship (fan characteristic), gas polytropic compression expansion process, unsteady air escape process, skirt-ground contact causing 'valving', and hysteretic behavior of the skirt material itself [4]. Joon Chung et. al. released a body of work about models of linear and nonlinear heave dynamics through a lumped-parameter bag and finger model [5], [6].

[1] ECE Department, Northeastern University, Boston, MA 02115. emails: miller.jare@husky.neu.edu, shafai@coe.neu.edu.

They present a two degree-of-freedom model with an inner and outer bag based on Lagrangian dynamics, where the nonlinearities in heave response are primarily observed with high input amplitudes. These nonlinearities include skirt contact forces, and chaotic behavior including sensitivity and period doubling are observed. Tae-Cheol Jung and Joon Chung use genetic algorithms in order to optimize the second peak magnitude with respect to the geometry of the skirt and ratio of bag and cushion pressure, and this optimization target ensures a perceived smooth ride [7], [8].

In 2012, Ahmed Sowayan and Khalid AlSaif presented equations of motion of the heave dynamics of air cushioned vehicles, focusing on open-skirted hovercraft hovering on a hard cushion of air [9], [10]. Their model synthesizes Newton's laws, Bernoulli's principle, and isotropic gas expansion to form a three-state model of heave dynamics (vertical height, velocity, and pressure directly under the hovercraft). They validate oscillatory behavior, find expressions of settling time in terms of dimensionless parameters, and perform a parametric study including Poincaré maps of chaotic pressure behavior under an increase in skirt length (heave does not exhibit chaos). The open skirt lacks bags or any method of retaining pressurized air, necessitating high mass inflow. This paper extends Sowayan and AlSaif's simplified three-state model to a bagged system, with air retention simulated by Forchheimer porosity.

This work is based on the 2017 Fall ECE Capstone competition, with the team from Paradigm Hyperloop. Paradigm was a collaboration between Northeastern University and Memorial University of Newfoundland to build and race an air-levitated pod for the SpaceX hyperloop competition. The pod stays aloft by expelling air through four air skates, and the cushioning effect of the pressurized air in bags provides a measure of protection from the ground/subtrack. Propulsion would be performed by either gas expulsion out of the back or linear induction motors on the track, and the air cushions would be bolstered by funneling incoming air underneath the pod to produce lift. Upon first activation of the skates, the pod exhibited significant oscillations. Although these were tuned out of the system during successive iterations of the technology, they were shown to still exist to a lesser extent during vacuum testing. While the capstone project aimed to create a full distributed hardware control system of a hyperloop pod, this work focused on creating and validating a dynamic model of pod motion in order to diagnose and fix the oscillations.

II. Heave Dynamics Model

Paradigm Hyperloop pod 2 is kept aloft by four air skates. Each air skate is composed of three valves to provide air, a series of diffusion layers, and a perforated nylon fabric facing the outside. When air flows through the system, the bag inflates and the net pressure difference keeps the pod up. Throughout this process, the majority of the bag is touching the ground.

Fig. 1: Pod 2 levitation and air supply subsystems. Further information about the pod available at https://paradigmhyperloop.com/. Images from Competition 2 used with permission.
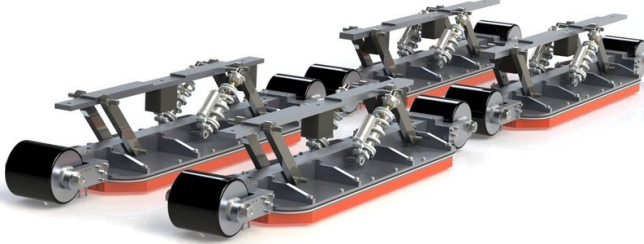
(a) The four air skates of the pod. Grey springs and black wheels are suspension elements, the red rim is the nylon bag that retains pressurized air. Bag is stretched over an HDPE bezel that forms an air cavity, and foam in the bezel forms the porous layer. Bag is pierced by a grid of small holes to form impingement (Forchheimer) effects. Air enters through the top ($\dot{m}_{in}$), stays in the bag chamber (p), and exits through the sides of the bag ($\dot{m}_{escape}$). The ride height z is the height of the inflated bag.
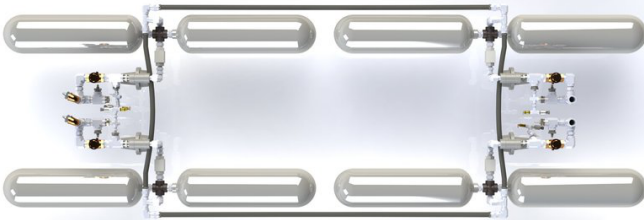
(b) Air supply that enables levitation, provides the skates with a total of $\dot{m}_{in} = 0.16 kg/s = 288.04 scfm$. Comprised of eight scuba tanks anchored on a central manifold, air flow to the skates is controlled by proportional MPYE flow regulator valves.

A. Model Derivation

This is a nonlinear system with three states: the height of the skate z, the vertical speed of the skate $\dot{z}$, and the pressure inside the bag p. The height of the bag changes through gravity and the gauge pressure of the bag. In reality, the equation $F = PA$ is invalid due to a nonuniform pressure distribution, but this is an acceptable approximation. This forms the first equation of motion:

$$ M\ddot{z} = (p - p_{atmo})A - Mg $$

Here, M is the mass of the pod, p_{atmo} is the outside pressure (101 kPa at atmosphere or 0.66 kPa at tube pressure) and A is the area of the skate. If there are multiple skates, then all quantities are treated as net ($A_{net} = N * A_{skate}$).

Equations of motion for the pressure inside the bag are more involved, and are at the heart of this study. Sowayan and Khalid's model uses Newton's second law, the compressible Bernoulli's equation, and nonlinear isentropic relations to form a 3-state model in $(z, \dot{z}, p)$ [9], [10]. The relevant equation governing the change in pressure $\dot{p}$ underneath the craft is given by:

$$ \dot{p} = \frac{\gamma RT}{V} \left(\dot{m}_{in} - \dot{m}_{out} - \frac{p\dot{V}}{RT} \right) $$

where the volume of the skate and its gradient are given by $V = Az$ and $\dot{V} = A\dot{z}$. The physical constants are the specific heat ratio of air $\gamma = c_p/c_v$, air temperature T, and ideal gas constant R. This equation shows that the change in pressure is proportional to the net mass flow in the volume which depends on applied mass flow $\dot{m}_{in} = u$, air escaping the bag $\dot{m}_{out}$, and the change in the mass of air due to changes in the bag volume $\frac{pA\dot{z}}{RT}$. Their paper uses the compressible Bernoulli equation to find the mass outflow, which results in:

$$ \dot{m}_{out} = \frac{c_0 pLz}{\sqrt{RT}} \left[\frac{2\gamma}{\gamma - 1} \left(\left(\frac{p_{atmo}}{p} \right)^{\frac{2}{\gamma}} - \left(\frac{p_{atmo}}{p} \right)^{\frac{\gamma+1}{\gamma}} \right) \right]^{\frac{1}{2}} $$

modified by an efficiency constant c_0. This expression is suitable for an skirted hovercraft, where there is no porous boundary layer between the pressurized air underneath the craft and the atmosphere. Simulation of this open-skirted approach has shown that the resultant ride height under $\dot{m}_{in}^* = 0.16\frac{kg}{s}$ is 0.885 mm, and this equilibrium is unstable. Keeping aloft while remaining stable with an open skirt requires unreasonable values of $\dot{m}_{in}$ to compete with a high $\dot{m}_{escape}$, so adding porous bags underneath the air skates provide a means to retain pressurized air.

A first approximation for flow across a porous boundary can be modeled through Darcy's law:

$$ \dot{m}_{escape} \approx -\frac{\rho_{atmo}\kappa A_e}{\mu} \frac{\partial P}{\partial x} $$

Darcy's law is a linear relation between pressure gradient across the porous material and outgoing mass flow rate. κ is the porosity of bag and x is the bag thickness. Assuming that no air is lost through contact with the ground and air only escapes through the sides of the bag, the effective escape area is $A_e = Lz$ if the total skate perimeter is L. $\frac{\partial p}{\partial x}$ is the change in pressure across the porous medium of thickness ℓ, and is approximated by $(p - p_{atmo})/\ell$. The input to this system is the incoming mass flow $u = \dot{m}_{in}$, and the linearization of the Darcy system reveals a fast pole at $-40,000$ rad/s (Darcy approximation of airflow) and two slow poles at $-57.9\pm133i$ (heave motion). The Darcy equilibrium has a very low ride height at equilibrium (0.68 mm) since air quickly escapes the bag with $\dot{m}_{in} = 0.16 kg/s$. The oscillatory poles dominate system behavior with a vertical frequency of 21.17 Hz (a very choppy ride). The Darcy approximation does not match up with the physical system, as in reality the small holes in

the bag result in choking effects (impingement). Air needs to travel through the throat diameter, reducing net outflow. The retention is better modeled by Forchheimer's equation, which adds a quadratic penalty to mass flow [11].
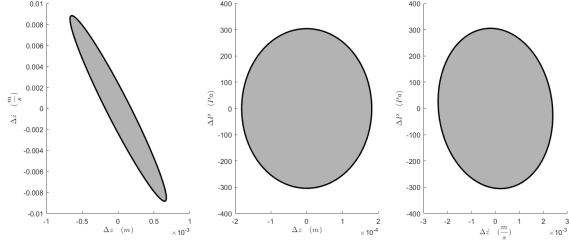

Fig. 2: Lyapunov Function $V(x)$'s invariant set certifying a region of stability for the pod in atmosphere (underestimate of true region of attraction). $V(x)$ found through the Lyapunov Equation $V(x) = x^T P x, P \geq 0, A^T P + PA + Q = 0$. Region of stability can be expanded through level set methods and bilinear optimization [12].

$$\rho_{atmo} \frac{\partial P}{\partial x} \approx \beta (\frac{\dot{m}_{escape}}{A_e})^2 + \frac{\mu}{\kappa}(\frac{\dot{m}_{escape}}{A_e})$$

where β is an inertia flow parameter which penalizes mass flow rate, μ is the viscosity of air at the given temperature, and κ is the porosity of the bag. The second-order term penalizes air escaping through the bag at a given height, meaning that an equivalent mass flow $\dot{m}_{in}$ will result in a higher ride height in the non-Darcy case vs. the linear Darcy. The non-Darcy model has greater levitation efficiency. Non-darcy flow as expressed by Forchheimer better approximates true pod dynamics, sliding the pole from s = -40,000 rad/s to -14.8 rad/s. The migrated non-Darcy pole at -14.8 rad/s dominates the oscillatory heave pole at -57.9 $\pm$ 133 rad/s, resulting in a smooth ride. The time constant of the system in pod liftoff is predicted to be 0.4 seconds, which exactly matches video of the pod. The equilibrium point predicted by Forchheimer's equation is stable for $\dot{m}_{in}^* = 0.16 \frac{kg}{s}$ in atmosphere, further verifying this model.

The accumulated equations of motion that describe the heave dynamics of the pod are:

$$M\ddot{z} = (p - p_{atmo})A - Mg \tag{1}$$
$$\dot{P}_{bag} = \frac{\gamma RT}{Az}(\dot{m}_{in} - \dot{m}_{escape} - \frac{pA\dot{z}}{RT}) \tag{2}$$

with arithmetic expressions:

$$\rho_{atmo}\frac{\partial P}{\partial x} = \beta(\frac{\dot{m}_{escape}}{A_e})^2 + \frac{\mu}{\kappa}(\frac{\dot{m}_{escape}}{A_e}) \tag{3}$$
$$A_e = Lz \tag{4}$$
$$\frac{\partial P}{\partial x} = \frac{p - p_{atmo}}{\ell} \tag{5}$$

where ℓ is the thickness of the bag's porous layer. The system has no zeros for z, but has one zero at $s = 0$ for $\dot{z}$ and two zeros at $s = 0$ for p, corresponding extremely roughly

to z as the double integral of pressure. The equilibrium ride height is a function of the applied mass flow rate $\dot{m}_{in}^*$. The mass flow equation can be reformulated as:

$$\frac{\beta}{L^2}\left(\frac{m_{in}^*}{z^*}\right)^2 + \frac{\mu}{\kappa L}\left(\frac{m_{in}^*}{z^*}\right) = \rho_{atmo}\frac{\partial P}{\partial x}$$

This equation can be solved for $\frac{m_{in}^*}{z^*}$. Given m_{in}^*, this equation can be used to find the resulting ride height z^*. Going the other way, a target z^* can be attained by supplying mass flow m_{in}^*. The bag pressure is constant $p^* = p_{atmo} + \frac{Mg}{NA}$ in order to support the weight of the pod, with the force required distributed over N bags.

Fig. 3: Pod simulations at atmospheric pressure (constant $\dot{m}_{in}$). Includes lifting off from ground and dropping from elevated position.
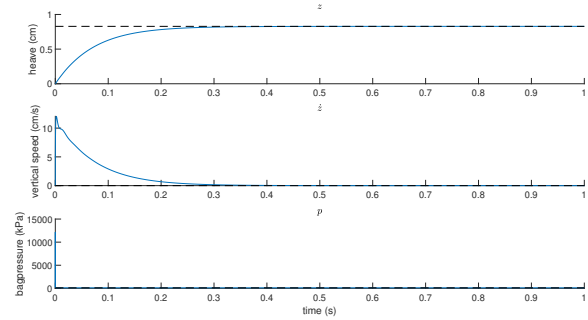

(a) Pod lifting off from the ground (actually 1e-10 m). The extraordinarily small volume coupled with a constant incoming mass flow rate results in a massive pressure spike at the beginning, which pushes the pod up. The velocity then starts to decrease, and gently pushes the pod to equilibrium. The time constant and exponential behavior is validated with respect to video footage of the pod.
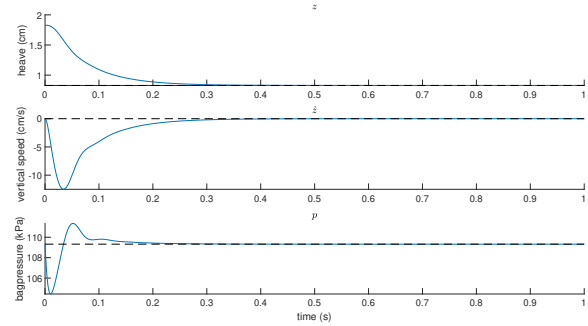
(b) Pod dropping from 1cm above equilibrium point. Volume is originally higher than equilibrium, so the pressure drops. At a certain critical point, the pressure reaches a minimum and starts to rise, slowing down the descent of the pod.

The above equations assume instantaneous response to a fluctuating $\dot{m}_{in}$. This is fine for constant mass inflow, but unrealistic for variable mass inflow. The flow controllers used on the pod are MPYE's from FESTO with a $G\frac{3}{8}$ pneumatic connection (part 151695) [13]. This controller has a critical frequency of 65 Hz = 408.4 rad/s, which adds a pole at $s = -408.4$ rad/s to all states. The lowpass filtering can be added to the model by adding a state $\dot{m}_{in}$:

Fig. 4: Simulation of the open-loop unstable heave dynamics of the pod at tube pressure. Oscillatory behavior is clearly observed as the pod lowers to the ground and bounces back up at ever greater amplitude.
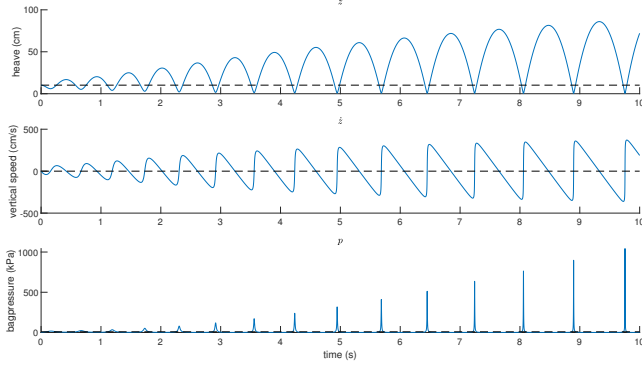

$$\ddot{m}_{in} = 408.4(\dot{m}_{in}^{\text{desired}} - \dot{m}_{in})$$

In a low pressure environment (0.66 kPa), the system physically starts to vibrate, and in the model become completely unstable. The non-Darcy pole moves to -12.3 rad/s, and the unstable heave dynamics are now $0.831 \pm 12.9i$ rad/s.

B. Disturbance Effects

The specific application of this system is to model heave dynamics of a hyperloop pod. In theory, these pods could reach speeds up to 400-600 mph. An air-levitated pod must remain stable even at speed, and the purpose of this section is to simulate practical disturbances entering into the heave model. As the pod is levitating against the ground/subtrack, the main disturbances under consideration are changes in the subtrack underneath the pod. The two disturbances will be changes in the subtrack height and gaps in the subtrack plates.

Fig. 5: Track profile including vertical drift and plate gaps
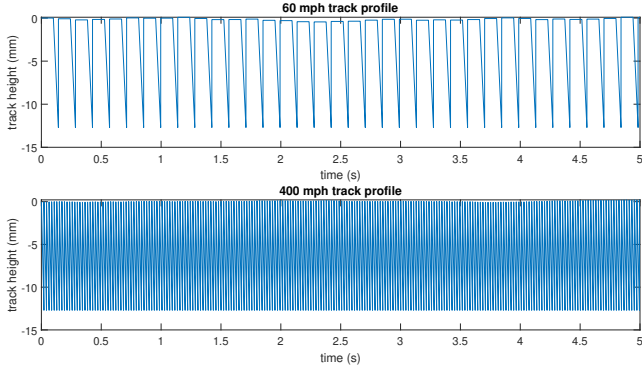
The track is made of a series of 12.5' plates, with a horizontal gap tolerance of 0.25". Between plates, there is also a vertical drift tolerance of ± 0.004" with a maximum accumulated drift of ± 0.4" away from nominal height [14]. The horizontal gap disturbance is w_{gap}, and a gap underneath the bag adds an area where air can escape. When $w_{gap} >$

0, m_{escape} will necessarily increase. Drifts in the vertical track height force a new equilibrium ride height, and pull down/push up the bottom of the bag (w_{height}). Intuitively, it is anticipated that a change in w_{height} will cause heave oscillations until the bag settles to the new equilibrium. The full equations of motion including effects of disturbances are described as follows:

$$M\ddot{z} = (P_{bag} - P_{atmo})A - Mg \quad (6)$$

$$\dot{p} = \frac{\gamma RT}{A(z + w_{height})}(\dot{m}_{in} - \dot{m}_{escape} - \frac{P_{bag}A\dot{z}}{RT}) \quad (7)$$

with arithmetic expressions:

$$\rho_{atmo}\frac{\partial P}{\partial x} = \beta(\frac{\dot{m}_{escape}}{A_e})^2 + \frac{\mu}{\kappa}(\frac{\dot{m}_{escape}}{A_e}) \quad (8)$$

$$A_e = L(z + w_{height}) + W w_{gap} \quad (9)$$

$$\frac{\partial P}{\partial x} = \frac{P_{bag} - P_{atmo}}{\ell} \quad (10)$$

w_{gap} is the length of the plate gap underneath the skate, so the total additional area exposed to air is $W w_{gap}$. A greater exposed area raises the outgoing mass flow rate of air, which in turn reduces the equilibrium ride height z^*. w_{height} is the height of each subtrack component, which does not effect the mass flow rate of air. Instead, it instantaneously changes the volume of the bag, and the bag responds accordingly. Given a track change w_{height}, the new equilibrium track height is $z^* \Leftarrow z^* + w_{height}$.

The generalized state space equation is $\dot{x} = Ax + B_w w + Bu$. In this case, x $= \begin{bmatrix} z & \dot{z} & P_{bag} & \dot{m}_{in} \end{bmatrix}^T$ $u = \dot{m}_{in}^{\text{desired}}$ and $w = \begin{bmatrix} w_{height} & w_{gap} \end{bmatrix}^T$. Pascals are inconveniently large as a unit, so the following linearization will use bar $= 10^5$ Pa with a change of basis matrix $T = \text{diag}\begin{bmatrix} 1 & 1 & 10^{-5} & 1 \end{bmatrix}$ in atmosphere (open-loop stable):

$$\dot{x} = \begin{bmatrix} 0 & 1 & 0 & 0 \\ 0 & 0 & 122.6 & 0 \\ -2521 & -184.8 & -130.6 & 130.5 \\ 0 & 0 & 0 & -408.4 \end{bmatrix} x \quad (11)$$

$$+ \begin{bmatrix} 0 & 0 \\ 0 & 0 \\ 2521 & -315.2 \\ 0 & 0 \end{bmatrix} w + \begin{bmatrix} 0 \\ 0 \\ 0 \\ 408.4 \end{bmatrix} u \quad (12)$$

The two disturbances are each L_∞ bounded, based on the geometry of the track (maximum gap and drift tolerance). If the underlying system is open loop stable, the influence of the disturbances are each Input to State Stable (ISS) [15]. The gap disturbance has extremely low energy due to the small gap width, and therefore has almost no effect on the pod's heave motion. As the pod velocity increases, it spends an almost negligible amount of time hovering over each gap, and each bag never spans more than one gap. The height disturbance is the major exogenous input of the system, and has the greatest effect on pod motion. All disturbances have the same poles and zeros as the original system when linearized, but with slightly different gains. The H_∞ norm

Fig. 6: Pod simulations at atmospheric pressure from 60-700mph with track irregularities (constant $\dot{m}_{in}$). Blue curves are pod states, dotted lines are track profile/disturbance.
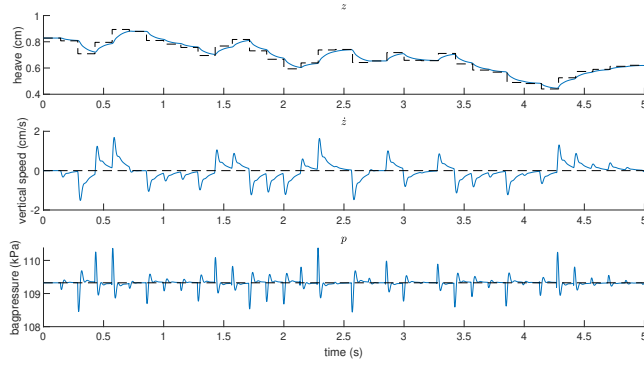
(a) Simulation of heave dynamics when the pod is traveling at 60mph. Step response to w_{height} is fast enough that the skate catches each height change, resulting in a bumpy ride.
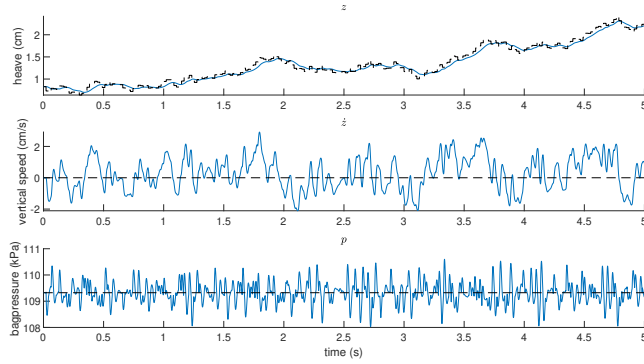
(b) Simulation of heave dynamics when the pod is traveling at 400mph. System is smoothing out step height changes. Similar to how driving a car quickly over a series of bumps leads to a gentle ride.
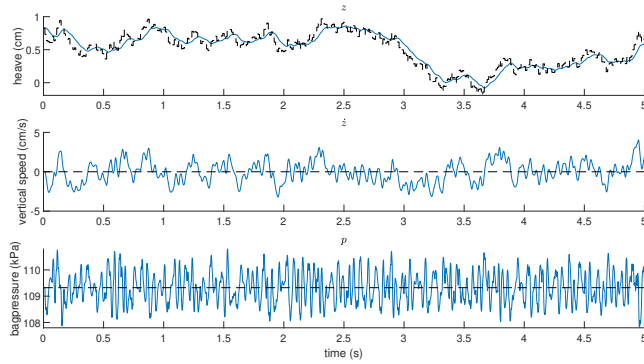

(c) Simulation of heave dynamics when the pod is traveling at 700mph. There is a noticeable lag between step height changes and response. There is a lowpass filtering effect inherent in the system rejecting the raised frequency of step height changes. Gaps continue to not effect the pod in any substantive way.

of the height disturbance is 20 times greater than the original system, and rangefinder sensors can only tell the disturbed position of the subtrack. The disturbance w_{height} fluctuates

so quickly at speed that there will not be enough time for a laser rangefinder on the pod to compute the altitude difference and the bag to inflate to a proper level. Even at nominal conditions, an active control system to reject disturbances of w_{height} and w_{gap} is doomed to failure, and a passive suspension-like approach is the way forward.

Fig. 7: Closed loop control of air skate system at tube pressure (0.667 kPa). Controller synthesized by LQR with $(q = [10, 10, 10, 100], r = 100)$. System is stabilized at $z^* = 13$cm and $\dot{m}_{in} = 0.21$ kg/s. The model clearly breaks down in low pressure cases.
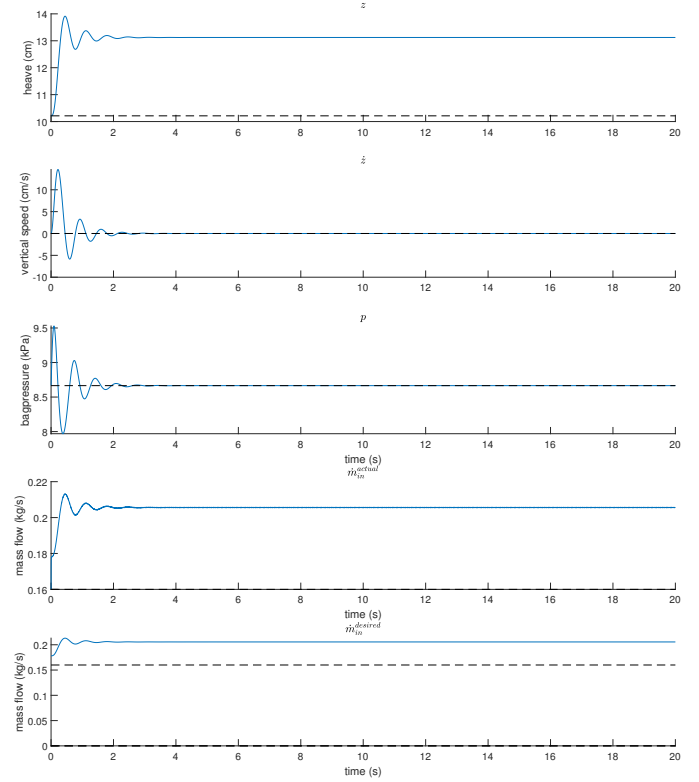
C. Issues with the Model

True dynamics of the hyperloop pod require a full solution of the Navier-Stokes equations. This model of motion ignores spatial dependence of the velocity field and pressure distributions, which give rise to interesting partial differential equations [16] (at steady state they appear like anti-helmholtz equations). Full spatial dependence will show that in a puck model (no bag), gauge pressure vanishes at the sides of the bottom face. In terms of the bag model, this involves fluid travelling between two plates, and air will probably more easily escape the center than the boundaries. When the pod is moving, Couette and Poiseuille flow will lower the outside pressure and change $\dot{m}_{escape}$ [17]. Couette flow also provides a drag force, not to neglect the drag coming from the shearing of the nylon bag on the ground. All simulations were performed with constant velocity, and acceleration/deceleration will assuredly change the response to disturbances. The quadratic Forchheimer flow rate is a

rough guess of the true behavior, and testing needs to be done to emperically determine the κ and β parameters. The model treats z as the top of the bag, and ignores the bottom of the bag. In reality, the nylon bag has an elasticity that resists stretching (E = 2-4 GPa), which also means under a height disturbance that the bag may fall towards the new track height and slowly increase the bag volume. Contact forces are also neglected, in which a sufficiently high w_{height} may cause the track to crash into the outside of the skate, rather than the change in height being absorbed and dissipated by the bag. A large decrease in w_{height} may cause the bag to no longer remain in contact with the ground, so air may escape from the bottom of the bag as well as the sides. This contact model is a hybrid system, and would exhibit oscillatory 'valving' behavior as described by Hinchey [4]. At sufficiently high speeds, frictive forces on the nylon bag may tear the bag, reducing levitation efficiency and returning the system to the skirted model. The model also neglects the variable mass of the system (as air gets expelled to provide lift), but the relatively modest $\dot{m}_{in} = 0.16 kg/s$ is overshadowed by the much larger pod mass of $909 kg$. This bagged heave dynamics model is an comparatively simple approximation to the true dynamics of air levitation, and it is remarkable that it performs as well as it does in atmosphere.

TABLE I: Environmental and System parameters of the Heave Dynamics Model

Variable	Quantity	Value	Units
l	Skate Length	0.9144	m
W	Skate Width	0.3048	m
N	Number of Skates	4	1
A	Total Skate Area	1.1148	m^2
L	Total Skate Perimeter	9.7536	m
M	Pod Mass	909	kg
g	Gravitational Acceleration	9.81	$\frac{m}{s^2}$
$\dot{m}_{in}^*$	Input Mass Flow	0.16	$\frac{kg}{s}$
z^*	Ride Height	8.28	mm
ℓ	Bag Thickness	2	mm
κ	Bag Permeability	1e-5	m^2
β	Forchheimer Coefficient	1.2e6	m^{-1}
μ	Air Viscosity	1.85e-5	$Pa*s$
T	Air Temperature	300	K
R	Specific gas constant of air	287	$\frac{J}{kg*K}$
γ	Air specific heat ratio	1.4	1
P_{atmo}	Atmospheric Pressure	101.325	kPa
ΔP_{bag}^*	Gauge Pressure of Bag	8	kPa
P_{tube}	Tube Pressure	0.666	kPa
ρ_{atmo}	Atmospheric Density	1.1768	$\frac{kg}{m^3}$

ACKNOWLEDGMENT

REFERENCES

[1] L. Yun and A. Bliault, *Theory and design of air cushion craft*. Elsevier, 2005.

[2] J. Wong, *Theory of Ground Vehicles*, ser. Wiley-Interscience. Wiley, 2001. [Online]. Available: https://books.google.com/books?id=LH8wd8im13AC

[3] J. Amyot, *Hovercraft technology, economics, and applications*, ser. Studies in mechanical engineering. Elsevier, 1989. [Online]. Available: https://books.google.co.uk/books?id=-LJTAAAAMAAJ

[4] M. Hinchey and P. Sullivan, "A theoretical study of limit cycle oscillations of plenum air cushions," *Journal of sound and vibration*, vol. 79, no. 1, pp. 61–77, 1981.

[5] J. Chung, "Theoretical investigation of heave dynamics of an air cushion vehicle bag and finger skirt," Ph.D. dissertation, National Library of Canada= Bibliothèque nationale du Canada.

[6] J. Chung and P. A. Sullivan, "Linear heave dynamics of an air-cushion vehicle bag-and-finger skirt," *Transactions of the Japan Society for Aeronautical and Space Sciences*, vol. 43, no. 140, pp. 39–45, 2000.

[7] T.-C. Jung and B. Eng, "Design of air cushion vehicles using artificial intelligence: Expert system and genetic algorithm," *Ann Arbor*, vol. 1050, pp. 48 106–1346, 2003.

[8] J. Chung and T.-C. Jung, "Optimization of an air cushion vehicle bag and finger skirt using genetic algorithms," *Aerospace Science and Technology*, vol. 8, no. 3, pp. 219–229, 2004.

[9] A. S. Sowayan and K. A. AlSaif, "Modeling of the transient response for compressible air cushion vehicles (acv)," in *Applied Mechanics and Materials*, vol. 152. Trans Tech Publ, 2012, pp. 560–567.

[10] ——, "Investigation of the heave dynamics of air cushion vehicles (acv): parametric and chaotic studies," *Latin American Journal of Solids and Structures*, vol. 10, no. 4, pp. 725–745, 2013.

[11] V. A. Jambhekar, "Forchheimer porous-media flow models-numerical investigation and comparison with experimental data."

[12] A. Majumdar, A. A. Ahmadi, and R. Tedrake, "Control design along trajectories with sums of squares programming," in *Robotics and Automation (ICRA), 2013 IEEE International Conference on*. IEEE, 2013, pp. 4054–4061.

[13] "Proportional directional control valves mpye," https://www.fhtperslucht.nl/uploaded_files-/FESTO_documentaties/MPYE_EN.PDF, 2012.

[14] "Spacex hyperloop test-track specification," Aug 2016. [Online]. Available: https://cdn.atraining.ru/docs/TubeSpecs.pdf

[15] E. D. Sontag, "Input to state stability: Basic concepts and results," in *Nonlinear and optimal control theory*. Springer, 2008, pp. 163–220.

[16] T. Witelski, D. Schwendeman, and P. Evans, "Analysis of pressurized porous air bearings," 2005.

[17] G. Stachowiak and A. Batchelor, *Engineering Tribology*, ser. Tribology series. Elsevier Science, 1993. [Online]. Available: https://books.google.com/books?id=yzxaPE1dwQkC